*Quantum Electronics* **46** (2) 150–154 (2016) 

DOI: 10.1070/QEL15879

# Gamma radiation-induced blue shift of resonance peaks of Bragg gratings in pure silica fibres

A.V. Faustov, A.I. Gusarov, P. Mégret, M. Wuilpart, D. Kinet, A.V. Zhukov, S.G. Novikov, V.V. Svetukhin, A.A. Fotiadi

*Abstract.* **We report the first observation of a significant gamma radiation-induced blue shift of the reflection/transmission peak of fibre Bragg gratings inscribed into pure-silica core fibres via multiphoton absorption of femtosecond pulses. At a total dose of ~100 kGy, the shift is ~20 pm. The observed effect is attributable to the ionising radiation-induced decrease in the density of the silica glass when the rate of colour centre formation is slow. We present results of experimental measurements that provide the key parameters of the dynamics of the gratings for remote dosimetry and temperature sensing.**

***Keywords:*** *fibre Bragg gratings, grating inscription by femtosecond pulses, radiation effects, remote sensing.*

## 1. Introduction

The general principle of fibre Bragg grating sensors is to measure the Bragg peak shift induced by changes in a parameter of interest. The advantages of such sensors, which determine their potential for use under various unfavourable conditions, include small dimensions, freedom from power supply and low sensitivity to electromagnetic fields. One adverse factor in space and nuclear industry facilities is radiation [1, 2], which influences parameters of Bragg gratings [3]. The most frequently mentioned unfavourable effect is the radiation-induced Bragg peak shift, which may reach hundreds of picometres. This effect may potentially be of interest for remote dosimetry [4–6], but in some instances it gives rise to measurement errors and should be reduced or completely eliminated. In connection with this, there is interest in gratings inscribed into pure silica fibre, which have low sensitivity to radiation and are thus better suited to temperature measurements in the presence of radiation. Because of the low sensitivity of silica glass to UV radiation, such gratings can only be written by femtosecond laser pulses, which may influence the radiation resistance of the gratings. Since femtosecond pulses have very high intensity ($\sim 10^{13}$ W cm$^{-2}$), absorption in fibre exposed to such pulses is the result of a multiphonon process, which leads to photochemical changes in the local structure of the silica glass [7, 8]. This grating inscription mechanism seems to be more general than classic inscription by UV exposure because it requires no photosensitive dopants or preliminary hydrogen loading. In particular, gratings can be written by femtosecond pulses both in fibres doped with various elements capable of improving their radiation sensitivity and in pure silica fibres, including photonic crystal fibres [9–11]. Moreover, gratings written by femtosecond pulses offer high thermal stability and can operate at temperatures of up to 1000 °C [12].

Radiation-induced changes in spectra of various types of gratings and for fibres of various compositions were described in a review by Gusarov and Hoeffgen [3]. Experimental data for gratings written using multiphoton absorption, in particular in germanium-doped fibres, demonstrate that the resonance wavelength (of their reflection/transmission peak) is an intricate function of ionising radiation dose [13, 14]. The behaviour of such gratings differs significantly from that of gratings written by low-intensity UV light [7]: in the latter case, gamma irradiation causes the peak of gratings written in doped fibres to shift monotonically to longer wavelengths because of the formation of colour centres, which increase the local refractive index [15]. A radiation-induced shift of peaks to shorter wavelengths was first observed by Maier et al. [16] in type IIa gratings. Such gratings are inscribed with a very long exposure, which causes appreciable damage. In other studies, however, a 'standard' shift to longer wavelengths was observed in type IIa gratings [3]. Moreover, Gusarov et al. [13] observed for the first time a blue shift in type I gratings. In a recent study, Butov et al. [17] also observed a blue shift of spectra of type I and IIa gratings that had been written in silica fibres with a nitrogen-doped core and held in contact with water during irradiation. The shift of the spectra, by several hundred picometres, exhibited threshold behaviour and was observed at radiation doses above about 200 kGy. The effect was accounted for under the assumption that the bonds produced by UV light during grating inscription were passivated with molecular hydrogen penetrating the glass. The hydrogen originated from water radiolysis in the course of the experiment [17]. At doses under 200 kGy, grating dynamics are difficult to probe by measurements in such experiments because of the insufficient accuracy in determining the resonance peak position (uncertainty above 20 pm).

In this paper, we report an experimental study of the dynamics of fibre gratings inscribed using a multiphoton

**A.V. Faustov** SCK•CEN, Boeretang 200, 2400 Mol, Belgium; University of Mons, place du Parc 20, 7000 Mons, Belgium;
**A.I. Gusarov** SCK•CEN, Boeretang 200, 2400 Mol, Belgium;
**P. Mégret, M. Wuilpart, D. Kinet** University of Mons, place du Parc 20, 7000 Mons, Belgium;
**A.V. Zhukov, S.G. Novikov, V.V. Svetukhin** Ulyanovsk State University, ul. L. Tolstogo 42, 432017 Ulyanovsk, Russia; e-mail: ZhukovAndreyV@mail.ru;
**A.A. Fotiadi** Ulyanovsk State University, ul. L. Tolstogo 42, 432017 Ulyanovsk, Russia; Ioffe Physical Technical Institute, Russian Academy of Sciences, Politekhnicheskaya ul. 26, 194021 St. Petersburg, Russia; University of Mons, place du Parc 20, 7000 Mons, Belgium

Received 10 June 2015; revision received 19 November 2015
*Kvantovaya Elektronika* **46** (2) 150–154 (2016)
Translated by O.M. Tsarev

absorption process into a radiation-hard pure silica fibre with a fluorine-doped cladding and exposed to gamma radiation at doses of 100 kGy or lower. In our experiments, which precluded temperature effects (during gamma irradiation, the temperature of the gratings was stabilised with a 0.1 °C accuracy), after a brief shift of the reflection/transmission peak of the gratings to longer wavelengths we observed a monotonic shift of the peak to shorter wavelengths. We present results of experimental measurements that provide the key parameters of the dynamics of the gratings exposed to gamma radiation and demonstrate the possibility of using the results in remote temperature sensing.

## 2. Experimental

In our experiments, we used gratings inscribed into segments of a radiation-hard pure silica fibre (Oxford Technology) having a core and fluorine-doped cladding about 4.5 and 125 μm in diameter, respectively (cutoff wavelength $\lambda_c$ = 1300 ± 20 nm, numerical aperture NA = 0.16). Type I gratings about 6 mm long were written in fibre sections stripped of their polymer coating, with no hydrogen loading. We used a phase mask with a period $\Lambda$ = 1070 nm and 120-fs pulses of the third harmonic (~266 nm) of a Ti : sapphire laser system (Spectra-Physics), which comprised an optical oscillator (Mai Tai) and amplifier (Spitfire Pro). The grating inscription conditions were described in detail elsewhere [18].

Figure 1a presents a schematic of the experiment. The fibre gratings to be tested (*2*) were fusion-spliced to telecom fibre leads (*1*,*3*) to form two fibre lines ~20 m in total length, which were connected to a Micron Optics si720 optical sensing analyser (*5*). The analyser enabled the reflection/transmission spectra of the gratings to be measured in the range 1520–1570 nm with a 1-pm absolute accuracy in wavelength and 0.2-pm reproducibility. During the measurements, the instrument was maintained at room temperature (20–23 °C). The fibre lines were enclosed in a flexible protective tube, and their central parts, including the gratings (*2*), were introduced into a specially designed chamber (*12*), equipped with active temperature stabilisation means (EuroTherm 3000 PID controller in combination with a thermocouple).

In our irradiation experiments, the chamber (*12*) was moved to the test zone and immersed in a water pool (*8*) to a depth of about 7 m, where the test fibre (*2*) was exposed to gamma radiation from external $^{60}$Co sources (*10*), with radiation field nonuniformity under 10%. Even though the fibre leads (*1*,*3*) were also exposed to radiation, the radiation-induced absorption in these fibres (less than 1 dB at the maximum gamma dose) had no effect on the measured Bragg resonance position of the gratings, because they did not require absolute intensity determination. Throughout the irradiation process, the temperature in the chamber (*12*) was maintained at a level $T$ = 30 °C with an accuracy $\Delta T$ = 0.1 °C, which ruled out any temperature effect on radiation measurements [19]. The dose rate around the test fibre (*2*) was $W$ = 420 Gy h$^{-1}$. The irradiation time was about 240 h. After irradiation, the chamber was lifted from the water pool and left on its surface for an additional 320 h. During this time period, the temperature in the chamber was not controlled and the gratings were subject to diurnal temperature variations.

## 3. Results and discussion

Figures 1b and 1c show transmission and reflection spectra of one of the gratings before and 320 h after irradiation. The grating has a fundamental resonance peak at a wavelength $\lambda_0 \approx$ 1540.93 nm. According to the transmission spectrum, the peak height is ~2.25 dB and the full width at half maximum of the peak is $\Delta\lambda \approx$ 160 pm. The reflection spectrum has a complex structure, with a large number of peaks, due to the finite grating length. The main peak is located at the same

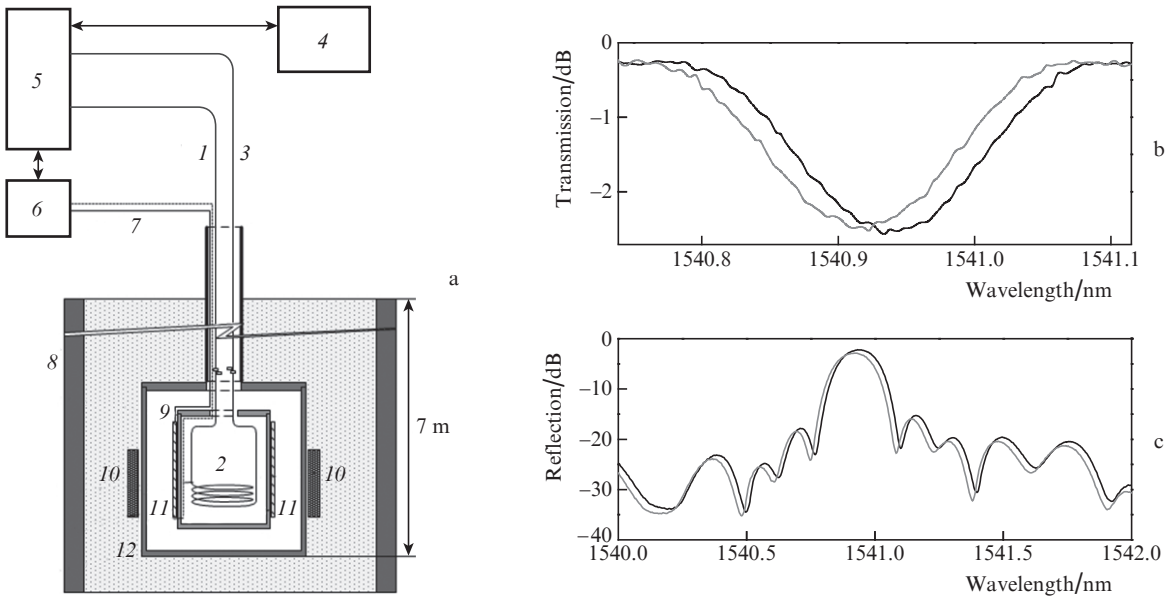


**Figure 1.** (a) Schematic of the experimental setup: (*1*–*3*) optical fibres; (*4*) computer; (*5*) spectrum analyser; (*6*) temperature controller; (*7*) thermocouple; (*8*) pool; (*9*) furnace; (*10*) $^{60}$Co sources; (*11*) heating elements; (*12*) irradiation container. (b) Transmission and (c) reflection spectra of the gratings before (black lines) and after (grey lines) irradiation. For convenience of comparison, the constant components of the spectra are omitted.

wavelength $\lambda_0$. Comparison of the spectra obtained before and after irradiation demonstrates that irradiation produces no significant changes in the height or width of the main peak, nor does the structure of the spectra change. At the same time, the spectra of the irradiated grating are shifted to shorter wavelengths ($\delta\lambda_0 \approx -20$ pm) relative to those of the unirradiated grating.

The other grating used in our experiments was written in a segment of the same fibre and under the same conditions. The gratings have identical initial spectral characteristics to within the accuracy in our measurements, so we present results for only one of them.

In radiation measurements, the reflection and transmission spectra of the gratings were taken alternately every 9 min. The Bragg resonance position was determined by fitting the main peaks with a Lorentzian (reflection peak) or Gaussian (transmission peak), which is a standard procedure for finding extrema of a spectrum [3] in data processing. To take into account the position of the peaks in both spectra at one data point (thereby reducing the noise component), we took the average over these two positions.

Figure 2a shows the time dependences of the experimentally determined Bragg peak shift $\delta\lambda_0$ for the two gratings. The gratings demonstrate identical dynamics to within the experimental accuracy in our measurements. During the first 2 h after the beginning of irradiation, the resonances shift to shorter wavelengths by –4 pm, which is followed by a shift to longer wavelengths. The maximum positive shift, about 2 pm, is reached after 7 h of irradiation, at an absorbed dose of 2.94 kGy. Further irradiation causes a monotonic shift of the resonances to shorter wavelengths by about 22 pm. The net negative shift during the whole period of irradiation, i.e. at an absorbed dose of ~100 kGy, is 20 pm, in perfect agreement with the data in Fig. 1b, obtained before irradiation and more than 320 h after. This means that all of the changes in the irradiated samples are persistent and cannot be annealed under the conditions described above.

In interpreting the present experimental data, we proceeded from the fact that shifts of Bragg resonances of fibre gratings are directly related to changes in the refractive index of the material of the optical fibres the gratings are written in. Indeed, the Bragg resonance wavelength is

$$\lambda_0 = 2\Lambda n_{\text{eff}}, \tag{1}$$

where $n_{\text{eff}}$ is the effective refractive index of the fundamental mode of the fibre, which is determined by the normalised mode power distribution $\rho(r)$ and local refractive index distribution $n(r)$ across the fibre:

$$n_{\text{eff}} = 2\pi \int_0^R \rho(r) n(r) r\,\mathrm{d}r \approx p_{\text{core}} n_{\text{core}} + p_{\text{clad}} n_{\text{clad}}. \tag{2}$$

Here $R$ is the radius of the fibre cladding, and $p_{\text{core}}$ and $p_{\text{clad}}$ are the fractions of the fundamental mode power in the core and cladding, which have local refractive indices $n_{\text{core}}$ and $n_{\text{clad}}$, respectively. Note that $n_{\text{clad}} < n_{\text{eff}} < n_{\text{core}}$ and $\Delta n = n_{\text{core}} - n_{\text{clad}} \approx 10^{-3}$ [12].

Irradiation may cause structural changes in fibre and/or the formation of colour centres (in both the core and cladding), which have a direct effect on the local refractive index $n(r)$, thereby changing $n_{\text{eff}}$ and, accordingly, the Bragg wavelength of the grating. Under the assumption that these mechanisms have additive effects on local refractive indices (or that they influence different regions in the cross section of the fibre), it is obvious from the experimental data in Fig. 2a that, during irradiation, at least two mechanisms are operative simultaneously. One mechanism prevails during the first few hours after the beginning of irradiation and leads to an increase in the effective mode index. The other becomes the main mechanism 10 h after the beginning of irradiation, at an absorbed dose of ~4.2 kGy, and leads to a decrease in $n_{\text{eff}}$. Since the overall Bragg resonance shift caused by the two mechanisms and measured during irradiation coincides with the shift measured before irradiation and a considerable time after, we are led to conclude that both mechanisms lead to persistent changes in the local refractive index $n(r)$.

To separately assess the contributions of the two mechanisms to changes in the effective mode index and confirm the above observations, we fitted the experimentally determined shifts $\delta\lambda_0$ (Fig. 2a) to exponential relations of the form $\delta\lambda_0 = A\exp(-t/T_{\text{r}}) + B$, which well represents the data obtained for the two gratings after irradiation for 10 or more hours, when the latter mechanism prevailed. According to the fitting results, the characteristic response time of the effective mode

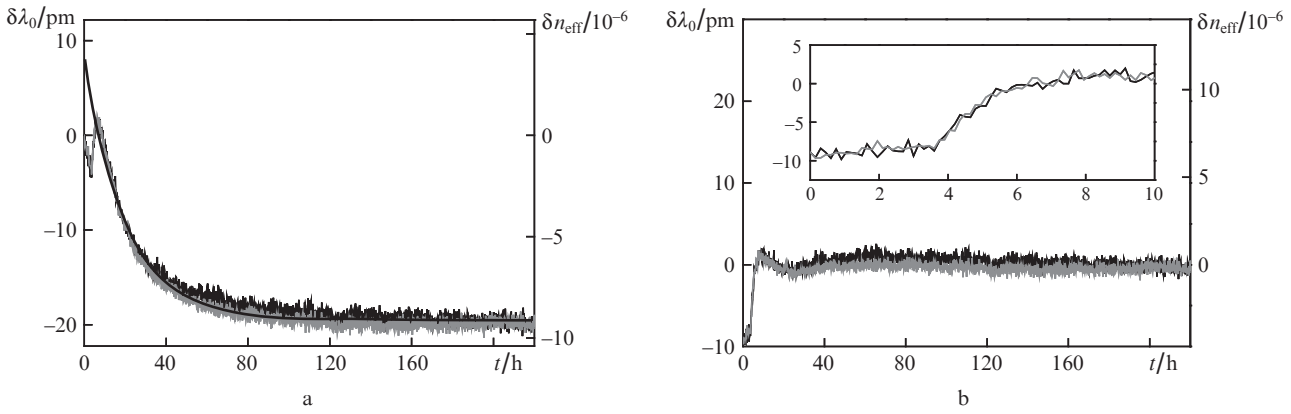


**Figure 2.** (a) Experimentally determined shifts of the Bragg resonances of the gratings and a fit with an exponential (black line); (b) difference between the experimentally determined shifts and the exponential fit. The right-hand vertical axis represents the variation of the effective refractive index of the fundamental mode of the fibre as assessed from the measured Bragg resonance shift: $\delta n_{\text{eff}} = \delta\lambda_0/2\Lambda$. The grey and dark grey lines refer to different gratings.

index is $T_r$ = 20.1 h, with $A$ = 28.4 pm and $B$ = –19.4 pm. In Fig. 2a, the exponential dependence is extended over the whole period of irradiation. During the first few hours after the beginning of irradiation, it represents the decrease in $n_{eff}$ due to the latter mechanism, whereas the former has the opposite effect. Accordingly, the former mechanism ensures an increase in the effective refractive index. After 5 h of irradiation, the effects of the two mechanisms exactly cancel each other, leading to zero Bragg resonance shift.

Figure 2b presents the same experimentally determined shifts after the subtraction of the exponential function shown in Fig. 2a. We believe that they should adequately describe the contribution of the former mechanism. It is well seen that this mechanism leads to a rapid rise in the refractive index during the first 5 h after irradiation, with saturation at a level corresponding to a positive Bragg resonance shift of +5 pm. The anomaly observed at the very beginning of irradiation suggests that this mechanism may also be contributed by several processes.

Thus, the observed behaviour of the gratings under irradiation can be understood in terms of additive effects of two competing mechanisms. The nature of these mechanisms has not yet been understood in sufficient detail, but the present experimental data provide an idea of their characteristic times and parameters. It is known that the presence of fluorine in silica glass does not lead to the formation of intrinsic colour centres and has only an indirect effect on the colour centres already present in the silica glass [20], in particular by relaxing strained Si–O–Si bonds. Most likely, the increase in $n_{eff}$ during the first few hours after the beginning of irradiation is due to the breaking of strained and unstable Si–O–Si bonds and the formation of nonbridging oxygen hole centres (NBOHCs), which have absorption peaks centred near 600 nm and are responsible for the radiation-induced absorption in the visible and IR spectral regions. This assumption is supported by the fact that the measured resonance shift dynamics represented in Fig. 2b are similar to the known dynamics of gamma radiation-induced absorption in fluorine-doped fibres: a rapid rise in absorption in the initial stage of irradiation, followed by saturation or even a decrease in absorption (in the case of 'wet' fibres) [21]. As to the latter mechanism, there is evidence that irradiation can reduce the density of silica glass [22]. In particular, this occurs when the silica glass network contains strained bonds. Irradiation of samples then leads to bond relaxation in Si–O–Si groups, thereby reducing the glass density, which is linearly related to the local refractive index $n(r)$. In our case, stress in the silica glass could be produced in the fibre fabrication process or in the course of grating inscription into the fibre using multiphoton absorption.

Figure 3a shows the Bragg resonance shifts measured for 320 h after irradiation, when the temperature in the chamber was not controlled. The resonance shift fluctuations are due to grating temperature oscillations. The measured temperature coefficients for both gratings are 103.4 °C nm$^{-1}$, in good agreement with previous data [3] (before irradiation, the coefficient was 100.7 °C nm$^{-1}$). Figure 3b presents the temperature difference extracted from these data for both gratings. The scatter in the data indicates that the error in our measurements did not exceed 0.4 °C.

## 4. Conclusions

We have studied the dynamics of fibre gratings written using multiphoton absorption of femtosecond pulses in segments of single-mode pure-silica fibre and exposed to gamma radiation. The reflection/transmission peak of the gratings has been shown to shift to shorter wavelengths. The shift is a monotonic, exponential function of absorbed dose (starting at $D \sim 3$ kGy), $\backsim \exp(-D/WT_r)$, with $WT_r \approx 8440$ kGy (without any noticeable restoration after irradiation). At an accumulated radiation dose of ~100 kGy, the shift to shorter wavelengths is ~20 pm. Such behaviour is characteristic of gratings inscribed into pure silica fibres, where the ionising radiation-induced formation of dopant-related colour centres is unlikely. The observed blue shift of the peak is most likely due to structural changes in the silica glass: a decrease in its density, which leads to a decrease in its refractive index. The absence of a backward shift of the peak after irradiation also indicates that the glass matrix undergoes persistent changes. The present results of experimental measurements provide the key parameters of the dynamics of the gratings for remote dosimetry and temperature sensing [19, 23, 24]. The accuracy in temperature measurements with the proposed experimental setup was about 0.4 °C. Accuracy can be significantly improved

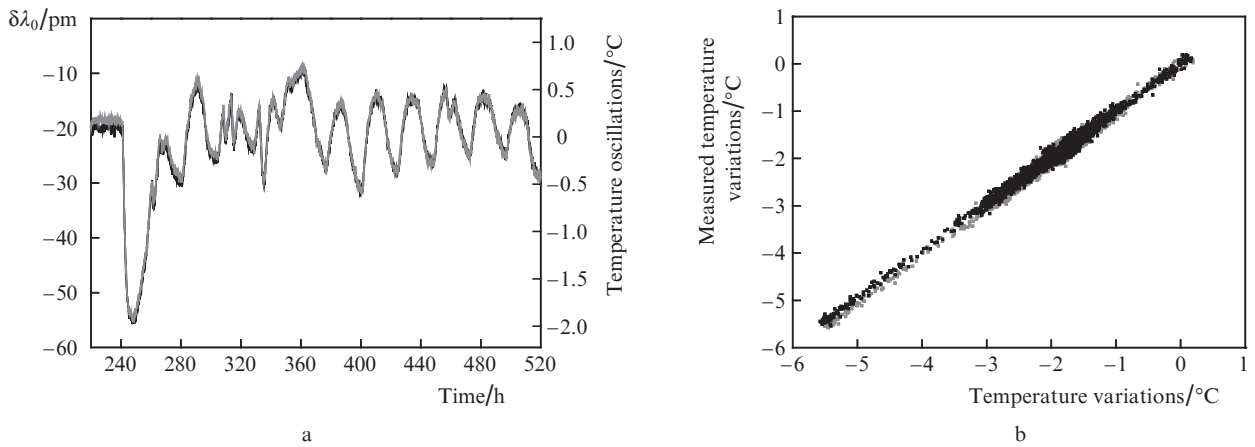


**Figure 3.** (a) Experimentally determined shifts of the Bragg resonances of the gratings, $\delta\lambda_0$, due to temperature fluctuations and (b) temperature variations relative to 30 °C evaluated from the measured shifts. The grey and black lines refer to different gratings.

by performing a larger number of independent measurements and using prediction–correction methods.

***Acknowledgements.*** This work was supported by the RF Ministry of Education and Science (Project No. RFMEFI57714X0074) and the Interuniversity Attraction Poles (IAP) Programme (Programme No. VII/35, Belgian Science Policy).

## References

1. Bergmans F., Gussarov A. In: *Fiber Bragg Grating Sensors: Recent Advancements, Industrial Applications and Market Exploitation* (Bentham Science Publishers, 2011).
2. Berghmans F., Brichard B., et al. In: *Optical Waveguide Sensing and Imaging* (Dordrecht, NL: Springer, 2008).
3. Gusarov A., Hoeffgen S.K. *IEEE Trans. Nucl. Sci*., **60**, 2037 (2013).
4. Henschel H., Köhn O., et al. *Nucl. Instrum. Methods Phys. Res., Sect. B*, **69**, 307 (1992).
5. Henschel H., Körfer M., et al. *Nucl. Instrum. Methods Phys. Res., Sect. A*, **526**, 537 (2004).
6. Krebber K., Henschel H., et al. *Meas. Sci. Technol*., **17**, 1095 (2006).
7. Nikogosyan D.N. *Meas. Sci. Technol*., **18**, R1 (2007).
8. Mihailov S.J., Smilser C.W., et al. *Lightwave Technol*., **22**, 94 (2004).
9. Brambillo G., Fotiadi A.A., et al. *Opt. Lett*., **31**, 2675 (2006).
10. Fotiadi A.A., Brambillo G., et al. *J. Opt. Soc. Am. B*, **24**, 1475 (2007).
11. Slattery S.A., Nikogosyan D.N., et al. *Proc. SPIE Int. Soc. Opt. Eng.*, **6187**, 618707 (2006).
12. Vasil'ev S.A., Medvedkov O.I. *Kvantovaya Elektron*., **35**, 1085 (2005) [*Quantum Electron*., **35**, 1085 (2005)].
13. Gusarov A., Kinet D., et al. *IEEE Trans. Nucl. Sci*., **57**, 3775 (2010).
14. Gusarov A., Brichard B., Nikogosyan D.N. *IEEE Trans. Nucl. Sci*., **57**, 2024 (2010).
15. Gusarov A., Vasiliev S., et al. *IEEE Trans. Nucl. Sci.*, **55**, 2205 (2008).
16. Maier R.R.J., MacPherson W.N., et al. *Proc. SPIE. Int. Soc. Opt. Eng.*, **5855**, 511 (2006).
17. Butov O.V., Golant K.M., Shevtsov I.A., Fedorov A.N. *J. Appl. Phys*., **118**, 074502 (2015).
18. Chah K., Kinet D., et al. *Opt. Lett.*, **38**, 594 (2013).
19. Faustov A., Gusarov A., et al. *Proc. SPIE Int. Soc. Opt. Eng.*, **8794**, 87943O (2013).
20. Kajihara K., Ikuta Y., et al. *Nucl. Instrum. Methods Phys. Res., Sect. B*, **218**, 323 (2004).
21. Kajihara K., Hirano M., et al. *Mater. Sci. Eng. B*, **161**, 96 (2009).
22. Raiaram J., Fribele E. *J. Non-Cryst. Solids*, **108**, 1 (1989).
23. Faustov A.V., Gusarov A. *Pis'ma Zh. Tekh. Fiz*., **41**, 6 (2015).
24. Faustov A., Gusarov A., et al. *IEEE Trans. Nucl. Sci.*, **60**, 2511 (2013).